Biosensors and Bioelectronics 26 (2011) 3037–3043

Contents lists available at ScienceDirect

Biosensors and Bioelectronics

journal homepage: www.elsevier.com/locate/bios

Covalent immobilization of cholesterol oxidase on self-assembled gold nanoparticles for highly sensitive amperometric detection of cholesterol in real samples

Urmila Saxena, Mitun Chakraborty, Pranab Goswami*

Department of Biotechnology, Indian Institute of Technology Guwahati, Guwahati 781039, Assam, India

ARTICLE INFO

Article history:
Received 14 September 2010
Received in revised form 1 December 2010
Accepted 3 December 2010
Available online 14 December 2010

Keywords:
Cholesterol oxidase
Covalent immobilization
Gold nanoparticles
Bioelectrode
Biosensor

ABSTRACT

A novel scheme for the fabrication of gold nanoparticle modified cholesterol oxidase based bioelectrode is presented and its application potential for cholesterol biosensor is investigated. The fabrication procedure is based on the deposition of gold nanoparticles on the 1,6-hexanedithiol modified gold electrode, functionalization of the surface of deposited gold nanoparticles with carboxyl groups using 11-mercaptoundecanoic acid and then covalent immobilization of cholesterol oxidase on the surface of gold nanoparticle film using the N-ethyl-N′-(3-dimethylaminopropyl carbodimide) and N-hydroxysuccinimide ligand chemistry. The assembly process of the bioelectrode is investigated using atomic force microscopy, cyclic voltammetry and electrochemical impedance spectroscopy. The gold nanoparticle film on the electrode surface provided an environment for the enhanced electrocatalytic activities and thus resulted in enhanced analytical response. The resulting bioelectrode is further applied to the amperometric detection of cholesterol and exhibited a linear response to cholesterol in the range of 0.04–0.22 mM with a detection limit of 34.6 μM, apparent Michaelis–Menten constant (K_m^{app}) of 0.062 mM and a high sensitivity of 9.02 μA mM^{-1}. The fabricated bioelectrode is successfully used for the selective determination of cholesterol in human serum samples.

1. Introduction

The fast and accurate determination of cholesterol has profound clinical applications since it is an important biomarker in the diagnosis of many diseases, such as hypertension, coronary heart disease, arteriosclerosis, lipid metabolism dysfunction, etc. (Aravamudhan et al., 2007). This has led to an increased interest in the development of various kinds of cholesterol biosensors as reviewed by Arya et al. (2008). Most of the cholesterol biosensors reported till date are based on the detection of electrooxidation of hydrogen peroxide produced during the catalysis of cholesterol by cholesterol oxidase (ChOx) (Turkarslan et al., 2009; Umar et al., 2009). This requires a high anodic potential (Iannello and Iacynych, 1981) that can induce simultaneous oxidation of other electrochemically active species present in samples leading to false positive signals. Therefore, in recent years, the focus of cholesterol biosensor research is being the direct electron transfer between its redox active site (FAD) and electrode surfaces (Willner et al., 2002). But deep embedment of FAD in the protein core prevents this direct electrical communication (Willner and Katz, 2000). Another common problem is that the total number of catalytically active immobilized enzyme units is usually small due to the random orientation and partial denaturation of the immobilized enzyme molecules on the electrode surface. As a result, cholesterol biosensors based on ChOx do not exhibit high signals leading to low sensitivity. Also, the poor compatibility of the support matrix may restrict the analytical efficiency of the developed biosensor (Sarma et al., 2009). Many efforts have been made for developing suitable support matrix that provides better environment for the efficient enzyme loading and maintenance of the enzymatic bioactivity so as to increase the sensitivity of the biosensor.

Varieties of nanoparticles, including metal nanoparticles and oxide nanoparticles have been widely used in constructing electrochemical biosensors (Li et al., 2006, 2010). Especially, gold nanoparticles (AuNPs) have been extensively used as enhancing interfacial platform for developing electrochemical sensors (Pingarron et al., 2008). The high surface area and a biocompatible microenvironment provided by the AuNP based matrices facilitate higher enzyme loading and help enzyme to retain its bioactivity, respectively (Crumbliss et al., 1992; Xiao et al., 1999; Yu et al., 2003). The excellent conductivity of the AuNPs makes them suitable for acting as "electronic wires" to enhance the transfer of electrons generated from the enzyme catalytic redox reaction to the elec-

* Corresponding author. Tel.: +91 361 2582202; fax: +91 361 2582249.
E-mail address: pgoswami@iitg.ernet.in (P. Goswami).

0956-5663/$ – see front matter © 2010 Elsevier B.V. All rights reserved.
doi:10.1016/j.bios.2010.12.009

trode surfaces (Bharathi et al., 2001; Willner et al., 2006) which in turn can decrease the overpotentials of many analytically important electrochemical reactions. These properties of AuNPs make them excellent candidate for replacing potentially harmful mediators in the construction of biosensors (Zhao et al., 1996).

Although AuNPs have been widely used for other biosensors, they are not adequately studied in case of cholesterol biosensors. Therefore the focus of the present investigation is to develop a suitable scheme for fabricating AuNP based cholesterol bioelectrode with improved stability and sensitivity. Among various enzyme immobilization approaches for the construction of AuNP based biosensors, technique based on electrostatic interaction has attracted much attention because of its simplicity in procedure (Yi et al., 2000). Although, AuNPs could efficiently adsorb proteins, the physical adsorption technique has a fatal drawback of reduced stability. Also, the random and non-optimized positioning of the proteins reduces the overall bioactivity of the adsorbed enzymes. Moreover, the property of ChOx being negatively charged in neutral pH (Wang and Mu, 1999) restricts its physical adsorption on materials with negative charge surface such as, citrate stabilized AuNPs. In the present study, ChOx molecules were covalently immobilized on the surface of AuNPs which were previously deposited on gold electrode using dithiol via Au–S bond. The electrochemical studies on the fabricated electrode demonstrated that incorporated AuNPs have a marked influence on the interface property of the modified electrode and played an important role in improving its current response.

2. Experimental

2.1. Chemicals and reagents

Cholesterol oxidase (EC 1.1.3.6 from *Pseudomonas fluoresens*, 24 U mg^{-1} solid), cholesterol esterase (ChEt) (EC 3.1.1.13 from *Pseudomonas* sp, 1.47 U mg^{-1} solid), peroxidase from horseradish (HRP) (1280 U mg^{-1} solid), cholesterol, gold (III) chloride solution (~30 wt.% in dilute HCl), N-ethyl-N′-(3-dimethylaminopropyl carbodimide) (EDC), N-hydroxysuccinimide (NHS), 1,6-hexanedithiol, and 11-mercaptoundecanoic acid (MUA) were bought from Sigma–Aldrich (USA). Cholesterol estimation kit was obtained from Merck. All other chemicals were of analytical grade. Human serum samples were collected from normal healthy volunteers.

Cholesterol stock solution of 10 mM was prepared in deionized water having 5% Triton X-100 and stored at 4 °C. Stock solution of ChOx (0.5 mg/ml) was freshly prepared in phosphate buffer solution (50 mM, pH 7.0) (PBS) and that of ChEt (1 mg/ml) in 400 mM phosphate buffer (pH 7) prior to being used.

AuNPs were prepared by the method of citrate reduction of gold (III) chloride solution in water at boiling temperature according to the literature (Frens, 1973; Turkevich et al., 1951). The formation of AuNPs was examined using the UV–vis spectrum, which shows a strong surface plasmon band at 530 nm (Supplementary S1 (A)). Transmission electron microscopy (TEM) analysis indicated average particle size of 20 nm (Supplementary S1 (B)). All solutions were prepared with deionized water (Millipore, Bedford, MA).

2.2. Fabrication of the bioelectrode

Scheme 1 shows the schematic diagram for the fabrication of the bioelectrode. A gold electrode (AuE) (diameter = 0.5 cm) was cleaned, first by polishing it with alumina powder, then washing it ultrasonically with 70% ethanol and water separately for 15 min each and finally drying in air. The cleaned AuE was dipped in 10 mM freshly prepared ethanolic solution of 1,6-hexanedithiol for 24 h. The dithiol modified electrode (AuE/dithiol) was rinsed with water and then dipped in freshly prepared AuNP solution for 6 h under mild shaking condition. The AuNPs modified electrode (AuE/dithiol/AuNPs) was rinsed with water and then dipped in 0.5 mM freshly prepared ethanolic solution of MUA for 5 h to obtain a layer of carboxylic group functionalized AuNPs. This AuE/dithiol/AuNPs/MUA electrode was treated with a solution of EDC (200 mM) and NHS (50 mM) for 10 min to activate the carboxylic group on the AuNPs. Then it was dipped in freshly prepared ChOx solution (10 mg/ml) for 12 h to obtain AuE/dithiol/AuNPs/MUA/ChOx bioelectrode. For preparing AuE/MUA/ChOx electrode, a cleaned AuE was first functionalized with MUA as above, treated with a solution of EDC (200 mM) and NHS (50 mM) for 10 min and then dipped in freshly prepared ChOx solution (10 mg/ml) for 12 h. The fabricated bioelectrodes were immersed in PBS for 15 min prior to being used.

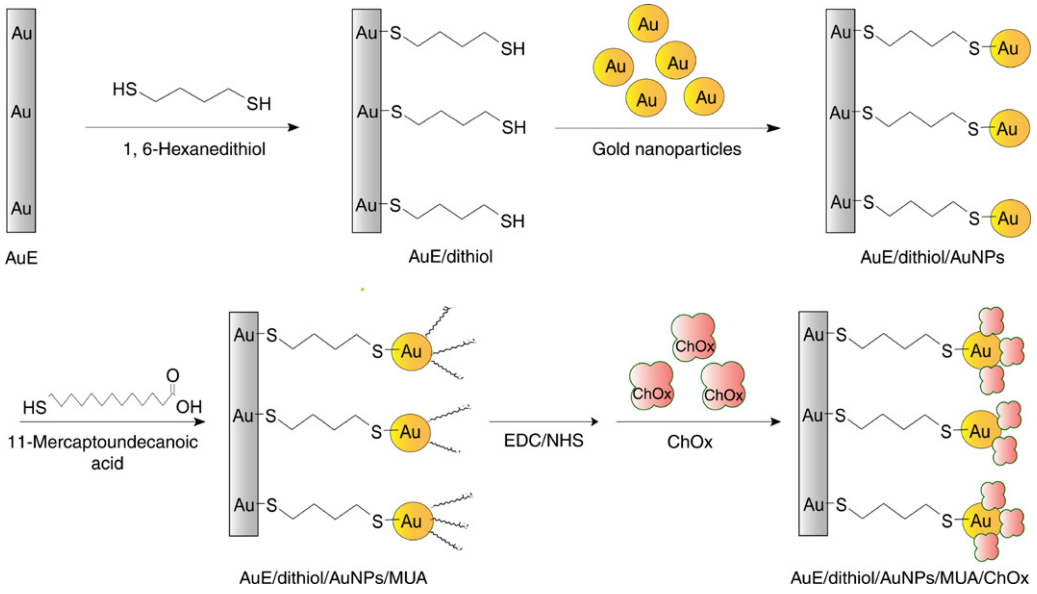

Scheme 1. Fabrication process of the AuE/dithiol/AuNPs/MUA/ChOx electrode.

The fabricated bioelectrodes were stored at 4 °C when not in use.

2.3. Apparatus and measurement

Cyclic voltammetry (CV) and electrochemical impedance spectroscopy (EIS) were performed with an Autolab PGSTAT 1212 (Eco Chemie, Netherlands). A three-electrode system was employed with platinum rod as counter electrode, Ag/AgCl (saturated KCl) as reference electrode, and gold electrode or modified gold electrodes as the working electrode. All potentials were measured and reported relative to the Ag/AgCl reference electrode. During the CV measurements, the electrolyte solution was constantly purged with argon gas. EIS measurements were performed in a background solution of 5 mM $K_3Fe(CN)_6/K_4Fe(CN)_6$ (1:1) and 0.1 M KCl in PBS within the frequency range of 0.05 Hz to 10 kHz. The amplitude of the alternate voltage was 5 mV. All experiments were performed at room temperature. Atomic force microscopy (AFM) was performed using an ambient air scanning probe microscope (Agilent Technologies 5500, USA). Images were recorded with typical contact mode using Picoscan 5 software.

The enzyme loading of the electrode was determined in terms of number of enzyme units retained per unit surface area ($U\,cm^{-2}$) of the electrode which in turn is calculated using a Sigma protocol of calculating ChOx activity with slight modifications. In brief, the ChOx immobilized electrode was immersed and incubated for 10 min at room temperature in a reaction mixture containing cholesterol (0.5 mM), 5 μl HRP (1 mg/ml in PBS), 10 μl of 4-amino antipyrine (4-AAP) (0.1 M in deionized water), 60 μl phenol (0.1 M) in total 1 ml PBS. The electrode was removed and the appearance of quinoneimine dye formed during the reaction was measured at 500 nm using a Cary 100 UV–vis spectrophotometer (Varian, USA). The enzyme loading ($U\,cm^{-2}$) was calculated using the following formula:

$$U\,\mathrm{cm}^{-2} = \frac{\Delta A}{0.5\varepsilon_{500} a t}$$

where ΔA is the change in absorbance in time t of incubation of the ChOx immobilized electrode and a is the area of the electrode. The molar extinction coefficient of quinoneimine dye at 500 nm (ε_{500}) is taken as 13.78 $mM^{-1}\,cm^{-1}$.

3. Results and discussion

3.1. Morphological characterization of the fabricated bioelectrode with atomic force microscopy

AFM measurements were carried out to characterize the morphological changes of the electrode surface obtained after major steps of bioelectrode fabrication. Fig. 1(A) shows the representative 2D and 3D AFM images of the bare gold disc. Fig. 1(B) shows the AFM images of AuNPs attached to the dithiol-modified gold disc with the formation of numerous clusters the diameter of which varied from 20 to 100 nm distributed homogenously over the gold surface. Also, the surface of the AuE/dithiol/AuNPs film is rougher than that of bare gold disc (Fig. 1(A)). This provided a significant increase of effective electrode surface area relevant for greater immobilization of biomolecules. When ChOx was assembled on the AuNP modified gold disc, the AFM images further changed (Fig. 1(C)). The AuE/dithiol/AuNPs/MUA/ChOx disc surface shows aligned structures which are formed by the assembling of globular ChOx molecules on the AuNP cluster surfaces. The AFM images indicate that the enzyme was successfully incorporated on the immobilized AuNPs over the electrode surface. AFM image was also taken for an AuE/MUA/ChOx disc in which ChOx molecules were immobilized directly on the bare Au disc without an interfacial layer of AuNPs. For preparing such disc, the Au disc was first functionalized with MUA and then ChOx molecules were covalently immobilized on the modified surface using EDC and NHS. It can be observed that ChOx were immobilized on the functionalized bare disc as evident from Fig. 1(D).

3.2. Electrochemical characterization of the fabricated bioelectrodes

3.2.1. Cyclic voltammetry

CV of bare gold and modified gold electrodes was done in a solution of 5 mM $K_3Fe(CN)_6/K_4Fe(CN)_6$ (1:1) and 0.1 M KCl in PBS to monitor changes in their electrochemical behavior introduced at different steps of electrode modification (Fig. 2(A)). The CV at the bare gold electrode (AuE) shows a well defined electrochemical response for $Fe(CN)_6^{4-/3-}$ with a couple of redox peaks. After the electrode was modified with dithiol (Au/dithiol), the CV curve changed drastically and the peak currents at the

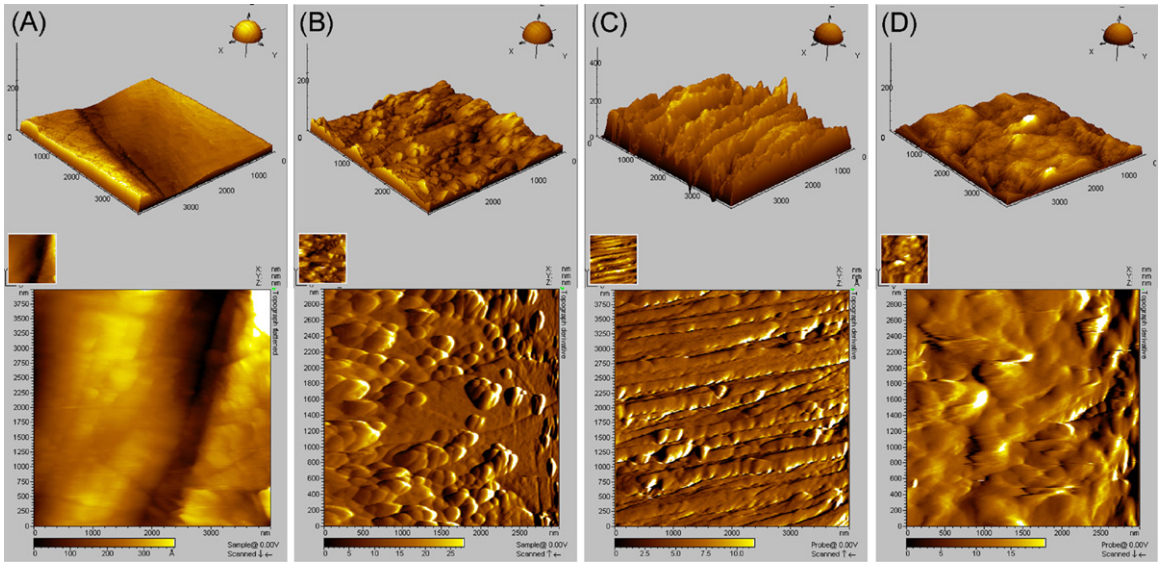

Fig. 1. AFM images of AuE (A), AuE/dithiol/AuNPs (B), AuE/dithiol/AuNPs/MUA/ChOx (C) and AuE/MUA/ChOx (D).

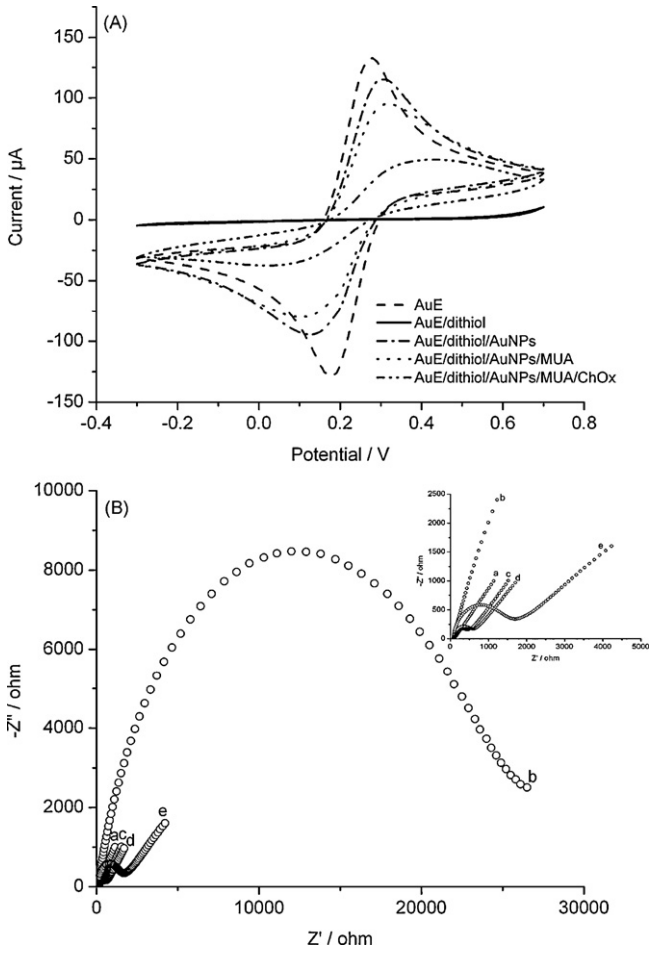

Fig. 2. (A) Cyclic voltammograms of AuE, AuE/dithiol, AuE/dithiol/AuNPs, AuE/dithiol/AuNPs/MUA and AuE/dithiol/AuNPs/MUA/ChOx electrodes in 5 mM $K_3Fe(CN)_6/K_4Fe(CN)_6$ (1:1) and 0.1 M KCl in PBS. Scan rate: 50 mV s^{-1}. (B) Electrochemical impedance spectra obtained at AuE (*a*), AuE/dithiol (*b*), AuE/dithiol/AuNPs (*c*), AuE/dithiol/AuNPs/MUA (*d*) and AuE/dithiol/AuNPs/MUA/ChOx (*e*) electrodes in 5 mM $K_3Fe(CN)_6/K_4Fe(CN)_6$ (1:1) and 0.1 M KCl in PBS. Inset: enlarged impedance spectra corresponding to curves (*a*), (*b*), (*c*), (*d*) and (*e*).

AuE/dithiol decreased dramatically in comparison with those of AuE. This may be due to the slow electron transfer kinetics through the negatively charged dithiol film. However, when AuNPs were self-assembled on the dithiol film (Au/dithiol/AuNPs), a quasi-reversible CV was obtained with increased peak currents. This shows that AuNPs have a marked influence on improving the conductivity of the modified electrode. Since the citrate stabilized AuNPs are negatively charged species, they repulse the negatively charged $Fe(CN)_6^{4-/3-}$ and interfere with the diffusion of ferricyanide towards the electrode surface and therefore, the observed peak current of AuE/dithiol/AuNPs is less than that of AuE. CV of AuE/dithiol/AuNPs/MUA electrode is almost similar with that obtained from AuE/dithiol/AuNPs electrode except a little decrease in the peak current. This indicates that the MUA does not have much effect on the electron transfer process of AuNPs because only the surface citrate ions are replaced by the MUA molecules and the overall surface charge density has not changed. CV of Au/dithiol/AuNPs/MUA/ChOx electrode shows a greatly diminished ferricyanide response and enlarged peak to peak separation which indicates that an insulating layer of ChOx is introduced.

3.2.2. Electrochemical impedance spectroscopy

EIS was employed to further monitor the interfacial properties on the electrode surface during the stepwise assembly of the bioelectrode. Fig. 2(B) shows the impedance spectra presented as Nyquist plots ($-Z''$ vs Z') obtained on different modified electrodes in a solution of 5 mM $K_3Fe(CN)_6/K_4Fe(CN)_6$ (1:1) and 0.1 M KCl in PBS. The value of the electron-transfer resistance (R_{et}) at the electrode surface can be estimated directly from the diameters of the high frequency semicircle. The impedance spectra of the bare AuE (curve *a*) consist of a small semicircle (R_{et}: 71 Ω) with an almost straight tail line, which is characteristic of a diffusional limiting step of the electrochemical process. The diameter of the high frequency semicircle was significantly increased (R_{et}: 26,000 Ω) by the surface deposition of the 1,6-hexanedithiol layer (curve *b*). This implies that the assembled dithiol film generated an obstruction to the electron transfer of the electrochemical probe at electrode surface. After the AuNPs were assembled on the dithiol film, the diameter of the high frequency semicircle was significantly reduced with a R_{et} value of 474 Ω (curve *c*), implying that AuNPs may play an important role in accelerating the electron transfer process. Since, the surface of the AuNPs is covered with a shell of citrate ions, therefore the R_{et} value of AuE/dithiol/AuNPs (curve *c*) is larger than that of AuE (curve *a*). The impedance spectrum of AuE/dithiol/AuNPs/MUA (curve *d*) was almost coincided with that of AuE/dithiol/AuNPs (curve *c*) with a R_{et} value of 586 Ω. This indicates that chemosorption of MUA molecules on AuNP surface did not have much effect on the electron transfer process. As shown in curve *e*, great increase in semicircular diameter of the impedance spectrum was found again when incubating the Au/dithiol/AuNPs/MUA electrode in a ChOx solution for 12 h indicating the formation of a ferrocyanide transport-blocking layer on the electrode. These results are consistent with that of CV experiments (Fig. 2(A)) implying that ChOx is successfully immobilized on a layer of AuNPs and AuE/dithiol/AuNPs/MUA/ChOx bioelectrode is developed.

3.3. Electrochemical response characteristics of AuE/dithiol/AuNPs/MUA/ChOx bioelectrode

CV was done in PBS for AuE and different modified gold electrodes at major steps of bioelectrode fabrication. No redox peaks were observed for bare AuE (Fig. 3(A) curve *a*) and AuE/dithiol/AuNP electrode (Fig. 3(A) curve *b*) whereas CV of AuE/dithiol/AuNPs/MUA/ChOx electrode shows a pair of redox peaks with a broad oxidation peak at around 0.46 V (Fig. 3(A) curve *c*). After the addition of cholesterol on AuE/dithiol/AuNPs/MUA/ChOx electrode, the anodic peak current at 0.46 V increased sharply (Fig. 3(B), curve *b*) as compared to that in the absence of cholesterol (Fig. 3(B), curve *a*). Thus, the oxidation peak at 0.46 V can be attributed to the electro-catalytic activity of ChOx. These results exhibit that ChOx gets electrically contacted with the AuNPs modified electrode. The electron transfer rates are highly sensitive to the type of self assembled monolayer (SAM) and the linking distance between the enzyme and the electrode surface (Benitez et al., 2004; Gooding et al., 2001). Thus, the overpotential (0.46 V) of ChOx may originate from the tunnelling barrier between the mixed SAM that is dithiol/AuNPs/MUA and the AuE surface. Addition of cholesterol also leads to an increase in current at around 0.7 V which is mainly because of H_2O_2 produced due to leaching of small amount of atmospheric O_2 inside the reaction chamber. Based on the Laviron's theory, the value of heterogenous electron transfer coefficient (k_s) of AuE/dithiol/AuNPs/MUA/ChOx electrode was calculated by measuring the variation of peak potential with scan rate (Laviron, 1979) and was found to be 0.35 s^{-1} which suggests significant electron transfer between the ChOx and the electrode.

In order to ascertain the influence of AuNPs, ChOx was immobilized on Au electrode via self-assembled monolayer of MUA without AuNPs (AuE/MUA/ChOx electrode). No clear oxidation peak was observed on AuE/MUA/ChOx electrode in absence (Fig. 3(C), curve *a*) or presence of cholesterol (Fig. 3(C), curve *b*). Different aspects

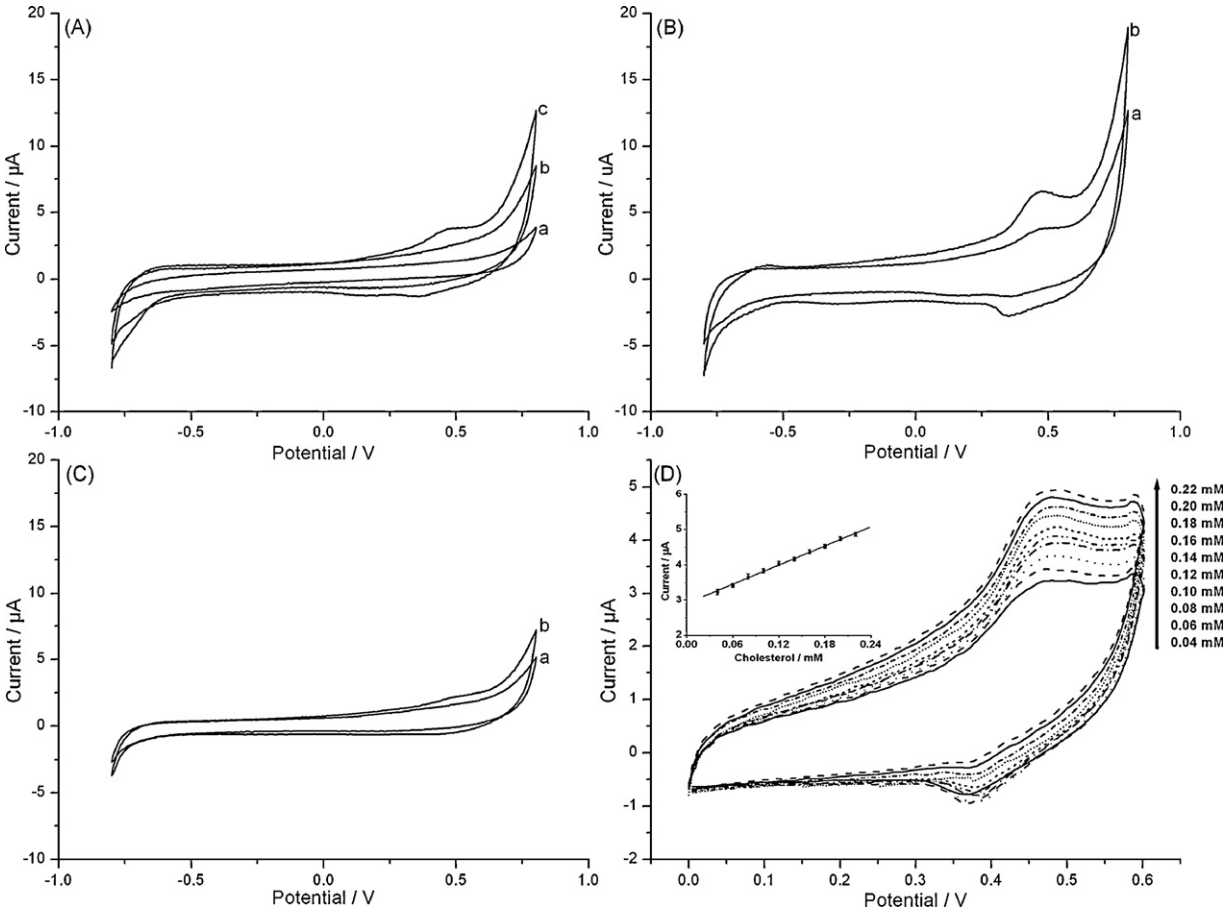

Fig. 3. Cyclic voltammograms of (A) AuE (*a*), Au/dithiol/AuNPs (*b*) and (*c*) Au/dithiol/AuNPs/MUA/ChOx electrode in PBS. (B) Au/dithiol/AuNPs/MUA/ChOx electrode in PBS in the absence (*a*) and in presence of 0.3 mM cholesterol (*b*). (C) Au/MUA/ChOx electrode in PBS in the absence (*a*) and in the presence of 0.3 mM cholesterol (*b*). (D) Au/dithiol/AuNPs/MUA/ChOx electrode in PBS with increasing concentrations of cholesterol. Inset of Fig. 4(D): calibration plot for Au/dithiol/AuNPs/MUA/ChOx electrode. Each datum point represents the average of the analysis of triplicate values ($n = 3$), with the range indicated with error bars. In all cases a potential scan rate of 0.1 V/s was used.

may account for this phenomenon. It is suggested that in absence of AuNPs, the total number of catalytically active ChOx units may be small due to comparatively lesser surface area and poor biocompatible environment provided by the bare gold electrode than the AuNP modified surface. To confirm this, enzyme loading was calculated on both AuE/dithiol/AuNPs/MUA/ChOx and AuE/MUA/ChOx electrodes and found to be 0.0037 U cm^{-2} and 0.00098 U cm^{-2}, respectively. There may be partial denaturation of the immobilized enzymes on the naked Au surface. The amount of immobilized electroactive enzyme was enhanced on incorporation of AuNPs. AuNPs can also provide conduction pathways to accelerate electron transfer and thus may act as the relayer of electrons to the electrode surface (Chen et al., 1998). Moreover, greater spatial freedom in the orientation of immobilized ChOx resulted in closer proximity of its redox center to electrode surface facilitating greater electron transfer. Thus, interfacial layer of AuNPs plays key role in enhancing the current response of the developed bioelectrode.

Fig. 3(D) shows the CVs of AuE/dithiol/AuNPs/MUA/ChOx bioelectrode in PBS with increasing concentrations of cholesterol. The calibration curve in Fig. 3(D) inset shows the peak current at 0.46 V increased linearly ($R^2 = 0.997$) with increase in cholesterol concentrations in the range of 0.04–0.22 mM. The sensitivity, calculated from the slope of the plot, was found to be 9.02 µA mM^{-1} (45.96 µA mM^{-1} cm^{-2}). The detection limit (DL) for the constructed bioelectrode calculated from the expression DL = (3 × SD)/sensitivity (where SD is the estimated standard deviation for the points used to construct the calibration curve and the sensitivity, its slope) was found to be 34.6 µM. The relative standard deviation (RSD) reflecting the accuracy of the measurement was determined by subjecting the same AuE/dithiol/AuNPs/MUA/ChOx bioelectrode to three different 0.2 mM cholesterol solutions and found to be 2.6%. A comparison of the analytical properties of the fabricated bioelectrode with those of other reported nanoparticles based cholesterol biosensors is given in Table 1. The apparent Michaelis–Menten constant (K_m^{app}) (based on Lineweaver–Burk plot) was calculated to be 0.062 mM which is better than those reported for other nanoparticle based cholesterol biosensors. This can be attributed to favorable conformation of ChOx provided by the AuNPs film. The detection range of the fabricated bioelectrode is wider as compared to cytochrome P450scc immobilized on AuNPs (Shumyantseva et al., 2005) but narrower than some other methods (Yang et al., 2006a; Matharu et al., 2009). The detection limit in our case is lower than ZnO NPs-CHIT composite (Khan et al., 2008) and SnO_2 NPs-CHIT (Ansari et al., 2009). The highest sensitivity of our fabricated bioelectrode among all the reported nanoparticle based cholesterol biosensors emphasizes the advantage of AuNP based electrode for cholesterol sensing over other matrices.

3.4. Practical usability of the bioelectrode

3.4.1. Interference studies

Effect of some common interferents in cholesterol determination such as ascorbic acid (AA), glucose (G), uric acid (UA), lactic acid (LA) and urea (U) on the AuE/dithiol/AuNPs/MUA/ChOx bio-

Table 1
Comparison of characteristics of AuE/dithiol/AuNPs/MUA/ChOx bioelectrode and other reported nanomaterial-based amperometric cholesterol biosensors.

Biosensor configuration	Sensing element	Method of immobilization	Linearity (mM)	Detection limit (μM)	Sensitivity	K_m^{app} (mM)	R.S.D. (%)	Stability (biosensor response retained)	References
MWCNTs-AuNPs-CHIT-IL	ChOx	Entrapment	0.5–5	n.r.[b]	200 μA M^{-1}	n.r.[b]	1.9	95% after 20 days[a]	Gopalan et al. (2009)
NiNP-CNTs	ChOx	Cross-linking	0.005–3	1	n.r.[b]	n.r.[b]	5.8	85% after 1 month	Yang et al. (2006a)
CNTs–PtNPs-CHIT	ChOx/ChEt	Cross-linking	0.01–3	5	n.r.[b]	n.r.[b]	5.4	90% after 1 week	Yang et al. (2006b)
AuNPs	ChOx	Physical adsorption	0.001–0.05[a]	0.005[a]	n.r.[b]	n.r.[b]	n.r.[b]	n.r.[b]	Zhou et al. (2006)
AuNPs	CYPP450scc	Physical adsorption	0.01–0.07[a]	10	0.13 μA μM^{-1}	n.r.[b]	n.r.[b]	n.r.[b]	Shumyantseva et al. (2005)
ZnO NPs-CHIT	ChOx	Entrapment	0.129–7.758[a]	129[a]	4.388 μA μM^{-1}[a]	0.22[a]	n.r.[b]	75% after 8 weeks	Khan et al. (2008)
PtNPs-CNTs	ChOx	Entrapment	0.004–0.1[a]	n.r.[b]	n.r.[b]	n.r.[b]	n.r.[b]	94.3% after 6 weeks	Shi and Peng (2005)
SnO_2 NPs-CHIT	ChOx	Physisorption	0.26–10.4[a]	130[a]	1.33 μA μM^{-1} cm^{-2}[a]	3.8	n.r.[b]	95% after 4–6 weeks	Ansari et al. (2009)
AuNPs-ODA octadecylamine	ChOx	Covalent attachment	0.65–13[a]	608[a]	1.085 μA mM^{-1}	n.r.[b]	n.r.[b]	~90% after 2 months	Matharu et al. (2009)
ZnO NPs	ChOx	Physical adsorption	0.000001–0.0005[a]	0.00037[a]	23.7 μA μM^{-1} cm^{-2}[a]	4.7	n.r.[b]	91.8% after 50 days	Umar et al. (2009)
AuE/dithiol/AuNPs/MUA/ChOx	ChOx	Covalent attachment	0.04–0.22	34.6	9.02 μA μM^{-1} (45.96 μA μM^{-1} cm^{-2})	0.062	2.6	~95% after 1 month	Present work

Abbreviations: MWCNTs, multiwalled carbon nanotubes; AuNPs, gold nanoparticles; CHIT, chitosan; IL, ionic liquid; NiNP, nickel hexacyanoferrates nanoparticles; CNTs, carbon nanotubes; PtNPs, platinum nanoparticles; ZnO NPs, zinc oxide nanoparticles; SnO_2 NPs, tin oxide nanoparticles; ODA, octadecylamine; AuE, gold electrode; MUA, 11-mercaptoundecanoic acid; ChOx, cholesterol oxidase; ChEt, cholesterol esterase; CYPP450scc, cytochrome P450scc; R.S.D., relative standard deviation.

[a] Values are normalized for making the units uniform for better comparison.

[b] Not reported.

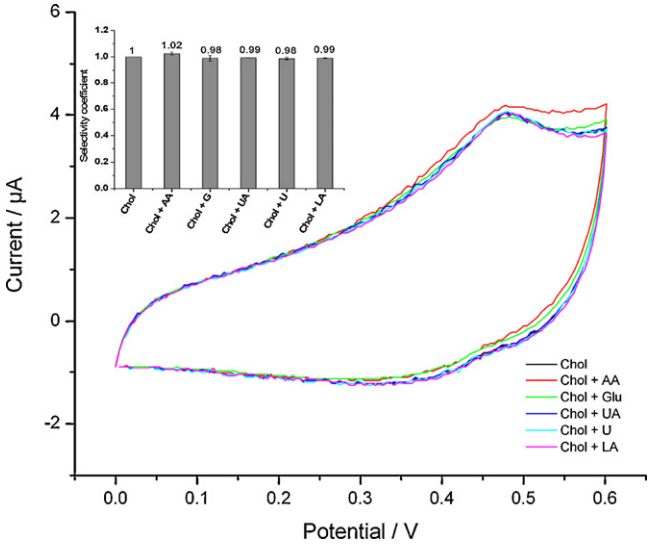

Fig. 4. Interference studies (Chol: cholesterol, AA: ascorbic acid, Glu: glucose, UA: uric acid, U: urea, LA: lactic acid). Each datum point represents the average of the analysis of triplicate values ($n = 3$), with the range indicated with error bars.

electrode response has been studied. For this, CVs were taken in PBS containing cholesterol (Chol) (0.2 mM) and each interferent (AA: 0.01 mM; G: 0.2 mM; UA: 0.01 mM; LA: 0.2 mM; U: 0.2 mM) individually (Fig. 4). Selectivity coefficient (SC) of the fabricated bioelectrode for each interferent was calculated using the formula, $SC = I_{c+i}/I_c$ where I_{c+i} and I_c are bioelectrode response at 0.46 V for cholesterol (0.2 mM) in the presence and absence of each interferents, respectively. The results indicate that response of bioelectrode did not get significantly affected due to presence of these interferents (Fig. 4). The concentration of AA and UA above 0.01 mM, significantly increased the oxidation current at 0.46 V. This may be due to the fact that both of them may be easily oxidized at electrodes. But the interference from these compounds become insignificant while analyzing real samples because of the dilution step involved during the amperometric measurements. These results show that AuE/dithiol/AuNPs/MUA/ChOx biosensor exhibited high selectivity towards the determination of cholesterol.

3.4.2. Determination of cholesterol in serum samples

The fabricated bioelectrode was used as a biosensor for determining total cholesterol content of human serum samples collected from five healthy volunteers. Serum samples were first analyzed using commercial cholesterol estimation kit (CHOD-PAP method) employing three enzymes, ChEt, ChOx and peroxidase, and 4-aminoantipyrine. In the CHOD-PAP method, ChEt first hydrolyzes the esterified cholesterol fraction into cholesterol and ChOx subsequently oxidizes the cholesterol liberating H_2O_2. Peroxidase utilizes H_2O_2 to convert 4-aminoantipyrine into quinoneimine (Trinder's reaction) (Trinder and Webster, 1984) detected spectrophotometrically at 500 nm. The same serum samples were analyzed using the AuE/dithiol/AuNPs/MUA/ChOx bioelectrode. Before the measurement, the serum samples were pretreated by mixing it with ChEt (1 mg/ml) in the presence of sodium cholate (0.75%) and Triton X-100 (0.1%) and incubating it at 37 °C for 30 min to hydrolyze the esterified cholesterol fraction followed by dilution with PBS (1:50) to make the cholesterol concentrations fall in the linear range of the bioelectrode. The dilution procedure can also reduce the interference effects. Current response for each sample was recorded at the working potential of 0.46 V and the cholesterol concentration was determined using the calibration curve (Fig. 3(D) inset). The cholesterol amount in all the serum samples determined with the bioelectrode and the cholesterol kit was compared using

paired *t*-test (Sigma 11) and the results show that there is no significant difference ($P = 0.920$) between the values obtained with both the methods. The results demonstrate that the fabricated bioelectrode can be used as a biosensor for precise determination of cholesterol in real samples.

3.5. Operational and storage stability of the bioelectrode

A freshly prepared AuE/dithiol/AuNPs/MUA/ChOx bioelectrode was taken and the variation in its current response towards cholesterol was monitored as a function of time and the number of measurements. For a period of 6 h, 30 measurements of a 0.2 mM cholesterol solution were performed by the bioelectrode. After each measurement, the bioelectrode was washed with PBS. Our results demonstrated that the bioelectrode still maintained 80% of its initial activity at the end of 30 measurements. The storage stability of AuE/dithiol/AuNPs/MUA/ChOx bioelectrode has been determined by measuring change in its current response for a 0.2 mM cholesterol solution at regular interval of 1 week for about 1 month. This AuE/dithiol/AuNPs/MUA/ChOx bioelectrode is stored at 4 °C in PBS when not in use. It has been found that the bioelectrode retained ~95% of its initial response after 1 month. Good operational and storage stability is attributed to the covalent attachment of the ChOx molecules with the AuNPs which prevents the leakage of the enzyme from the electrode surface.

4. Conclusions

A novel scheme for the fabrication of ChOx and AuNPs based bioelectrode has been developed. The self-assembled AuNPs on the gold electrode was found to enhance the current response of the fabricated bioelectrode by increasing the electroactive surface area for higher enzyme loading, providing a biocompatible environment for the ChOx and improving the conductivity of the electrode surface. The fabricated bioelectrode shows a favorable effect on the electrochemical oxidation of cholesterol and at the same time maintaining the good bioactivity of the immobilized ChOx. The covalent attachment of the ChOx to the AuNPs provided high stability of the bioelectrode. The bioelectrode was also demonstrated to be effectively used as an amperometric biosensor for the determination of cholesterol in real samples. Therefore, taking into account the good performance of the fabricated bioelectrode, the proposed fabrication method is of great interest for the development of highly sensitive and stable nanostructured biosensors.

Acknowledgements

We acknowledge the financial assistance from Department of Biotechnology (DBT), India and Council of Scientific and Industrial Research (CSIR), India. We acknowledge CIF, IITG for providing AFM facility.

Appendix A. Supplementary data

Supplementary data associated with this article can be found, in the online version, at doi:10.1016/j.bios.2010.12.009.

References

Ansari, A.A., Kaushik, A., Solanki, P.R., Malhotra, B.D., 2009. Electroanalysis 21, 965–972.
Aravamudhan, S., Ramgir, N.S., Bhansali, S., 2007. Sens. Actuators B 127, 29–35.
Arya, S.K., Datta, M., Malhotra, B.D., 2008. Biosens. Bioelectron. 23, 1083–1100.
Benitez, G., Vericat, C., Tanco, S., Lenicov, F.S., Castez, M.F., Vela, M.E., Salvarezza, R.C., 2004. Langmuir 20, 5030–5037.
Bharathi, S., Nogami, M., Ikeda, S., 2001. Langmuir 17, 1–4.
Chen, X., Li, J., Li, X., Jiang, L., 1998. Biochem. Biophys. Res. Commun. 245, 352–355.
Crumbliss, A.L., Perine, S.C., Stonehuerner, J., Twberge, K.R., Zhao, J., Henkens, R.W., O'Daly, J.P., 1992. Biotechnol. Bioeng. 40, 483–490.
Frens, G., 1973. Nat. Phys. Sci. 241, 20–22.
Gooding, J.J., Erokhin, P., Losic, D., Yang, W., Policarpio, V., Liu, J., Ho, F.M., Situmorang, M., Hibbert, D.B., Shapter, J.G., 2001. Anal. Sci. 17, 3–9.
Gopalan, A.I., Lee, K.P., Ragupathy, D., 2009. Biosens. Bioelectron. 24, 2211–2217.
Iannello, R.M., Iacynych, A.M., 1981. Anal. Chem. 53, 2090–2095.
Khan, R., Kaushik, A., Solanki, P.R., Ansari, A.A., Pandey, M.K., Malhotra, B.D., 2008. Anal. Chim. Acta 616, 207–213.
Laviron, E., 1979. J. Electroanal. Chem. 101, 19–28.
Li, J., Yuan, R., Chai, Y., Che, X., 2010. J. Mol. Catal. B: Enzymol. 66, 8–14.
Li, Y.F., Liu, Z.M., Liu, Y.L., Yang, Y.H., Shen, G.L., Yu, R.Q., 2006. Anal. Biochem. 349, 33–40.
Matharu, Z., Pandey, P., Pandey, M.K., Gupta, V., Malhotra, B.D., 2009. Electroanalysis 21, 1587–1596.
Pingarron, J.M., Yanez-Sedeno, P., Gonzalez-Cortes, A., 2008. Electrochim. Acta 53, 5848–5866.
Sarma, A.K., Vatsyayan, P., Goswami, P., Minteer, S.D., 2009. Biosens. Bioelectron. 24, 2313–2322.
Shi, Q.C., Peng, T.Z., 2005. Chin. Chem. Lett. 16, 1081–1084.
Shumyantseva, V.V., Carrara, S., Bavastrello, V., Riley, D.J., Bulko, T.V., Skryabin, K.G., Archakov, A.I., Nicolini, C., 2005. Biosens. Bioelectron. 21, 217–222.
Trinder, P., Webster, D., 1984. Ann. Clin. Biochem. 21, 430–433.
Turkarslan, O., Kayahan, S.K., Toppare, L., 2009. Sens. Actuators B 136, 484–488.
Turkevich, J., Stevension, P.C., Hiller, J., 1951. Disc. Faraday Soc. 11, 55–75.
Umar, A., Rahman, M.M., Al-Hajry, A., Hahn, Y.B., 2009. Talanta, 284–289.
Wang, H., Mu, S., 1999. Sens. Actuators B 56, 22–30.
Willner, B., Katz, E., Willner, I., 2006. Curr. Opin. Biotechnol. 17, 589–596.
Willner, I., Willner, B., Katz, E., 2002. Rev. Mol. Biotechnol. 82, 325–355.
Willner, I., Katz, E., 2000. Angew. Chem. Int. Ed. 39, 1180–1218.
Xiao, Y., Ju, H.X., Chen, H.Y., 1999. Anal. Chim. Acta 391, 73–82.
Yang, M., Yang, Y., Qu, F., Lu, Y., Shen, G., Yu, R., 2006a. Anal. Chim. Acta 571, 211–217.
Yang, M., Yang, Y., Yang, H., Shen, G., Yu, R., 2006b. Biomaterials 27, 246–255.
Yi, X., Huang-Xian, J., Hong-Yuan, C., 2000. Anal. Biochem. 278, 22–28.
Yu, A., Liang, Z., Cho, J., Caruso, F., 2003. Nano Lett. 3, 1203–1207.
Zhao, J., O'Daly, A.L., Henkens, R.W., Stomehurner, J., Crumbliss, A.L., 1996. Biosens. Bioelectron. 11, 493–502.
Zhou, N., Wang, J., Chen, T., Yu, Z., Li, G., 2006. Anal. Chem. 78, 5227–5230.